DMD Fast Forward. Published on September 30, 2005 as doi:10.1124/dmd.105.004929

STRUCTURAL ELUCIDATION OF HYDROXYLATED METABOLITES OF THE ISOFLAVAN EQUOL BY GC/MS AND HPLC/MS

Corinna E. Rüfer, Hansruedi Glatt, and Sabine E. Kulling

Institute of Nutritional Physiology, Federal Research Center for Nutrition and Food, Karlsruhe, Germany (C.E.R.)

Department of Nutritional Toxicology, German Institute of Human Nutrition, Potsdam-Rehbrücke, Germany (H.R.G.)

Department of Food Chemistry, Institute of Nutritional Science, University of Potsdam, Potsdam-Rehbrücke, Germany (S.E.K.)

Running title: Phase I metabolism of equol

Corresponding author:
Sabine E. Kulling
Arthur-Scheunert-Allee 114-116
Institute of Nutritional Science,
Department of Food Chemistry
University of Potsdam
14558 Nuthetal, Germany
Tel.: +49-33200/88-580; Fax: +49-33200/88-582
E-Mail: kulling@rz.uni-potsdam.de

Number of pages: 47
Number of tables: 1
Number of figures: 15
Number of references: 29
Number of words in the abstract: 183
Number of words in the introduction: 667
Number of words in the discussion: 915

Abbreviations used:

API-ES, atmospheric pressure electrospray ionization; BSTFA, *N,O*-bis-(trimethylsilyl)trifluoroacetamide; CYP, cytochrome P450; d9-BSA, deuterated *N,O*-bis-(trimethylsilyl)acetamide; EI-MS, electron impact ionization mass spectrometry; GC, gas chromatography; GC/MS, gas chromatography/mass spectrometry; HLM, human liver microsomes; HPLC, high performance liquid chromatography; $NADP^+$, β-nicotinamide adenine dinucleotide phosphate; NADPH, β-nicotinamide adenine dinucleotide phosphate, reduced form; rDA, retro Diels-Alder; SIM, selected ion monitoring; TMS, trimethylsilyl.

Abstract

Equol has - as other isoflavonoids - recently gained considerable interest due to its possible health effects. However, detailed studies on the metabolism of equol are scarce. Therefore, we investigated the phase I metabolism of equol using liver microsomes from Aroclor-treated male Wistar rats as well as from a male human. The identification of the metabolites formed was elucidated using high performance liquid chromatography (HPLC) with diode array detection, HPLC/atmospheric pressure ionization electrospray mass spectrometry, gas chromatography-mass spectrometry as well as reference compounds. (+/-)-Equol was converted to eleven metabolites by the liver microsomes from Aroclor pretreated rats comprising three aromatic monohydroxylated and four aliphatic monohydroxylated as well as four dihydroxylated products. The main metabolite was identified as 3'-hydroxy-equol. Using human liver microsomes, equol was converted to six metabolites with 3'-hydroxy- and 6-hydroxy-equol as main products. Furthermore the aliphatic hydroxylated metabolite 4-hydroxy-equol, which was recently detected in human urine after soy consumption, was formed. On the basis of these findings it is suggested that phase I metabolism of equol is part of a complex biotransformation of the soy isoflavone daidzein in humans in vivo.

Introduction

Equol (7,4'-dihydroxy-isoflavan) is a nonsteroidal estrogen of the isoflavone family. In 1932, Marrian et al. were the first who isolated equol from the urine of pregnant mares and elucidated its chemical structure. The equine origin gave the basis for its name (Marrian et al., 1932). Four decades later, in 1982, it was identified in human urine (Axelson et al., 1982). Equol was established as a bacterial metabolite of daidzein in 1968 (Shutt and Braden, 1968). It is one of the end products of the intestinal bacterial biotransformation of the isoflavone daidzein, which is one of the two predominant phytoestrogens found in soy and soy derived products (figure 1). Therefore, equol is not a phytoestrogen itself since it is no natural constituent of plants. Equol is unique in having a chiral center at C-3 due to the lack of a double bond in the heterocyclic C-ring. In vivo the absolute configuration of equol was determined to be S-(-)-equol (Setchell et al., 2005).

Only 30 - 50% of the adult population excretes equol in urine after having consumed soy foods (Rowland et al., 2000) - an observation which is still not understood. Even when pure daidzein is administered, which removes the influence of the food matrix, a high percentage of humans do not convert daidzein to equol. This phenomenon has led to the terminology of being an "equol-producer" or a "nonequol-producer" to describe the two distinct populations. Recently, the question arose whether "equol-producers" have particular benefit in the treatment and the prevention of hormone-dependent diseases by consuming soy products, since the biological properties of equol are interesting. Equol possesses high estrogenic activity: The binding affinities to both estrogen receptors, α and β, are similar to those of genistein with a preference for estrogen receptor β. However, equol induces binding of the activated receptor to the estrogen response element as well as transcription more strongly,

especially with estrogen receptor α (Morito et al., 2001; Kostelac et al., 2003; Muthyala et al., 2004). Recently, the binding affinities of R- and S-equol as well as the racemate to both estrogen receptors have been separately elucidated. Interestingly, S-equol possesses high binding affinity for estrogen receptor β, whereas R-equol binds less strongly and with a preference for estrogen receptor α (Muthyala et al., 2004). Equol can act as an anti-androgen by binding 5α-dihydrotestosterone with high affinity, which prevents 5α-dihydrotestosterone from binding the androgen receptor (Lund et al., 2004). Furthermore, equol has superior antioxidant properties compared to all other isoflavones (Arora et al., 1998; Turner et al., 2004).

The metabolism of soy isoflavones is well documented. Daidzein is reduced to dihydrodaidzein by the gut microflora, which is further metabolized to equol and *O*-desmethylangolensin (figure 1) (Chang and Nair, 1995; Joannou et al., 1995). Despite the growing interest in the biological properties of equol data on the pharmacokinetics and metabolism are scarce. There is only one study investigating the bioavailability of equol. Setchell and coworkers administered a single-bolus oral dose (25 mg) to one healthy adult (Setchell et al., 2002). Maximal plasma concentrations were attained after 4 - 6 h, the elimination half-life was determined to be 8.8 h. Equol exerted similar pharmacokinetic parameters to the other isoflavones, however, the plasma clearance in man was much slower compared to its parent compound daidzein (Cl/F = 6.9 L/h versus 17.5 L/h). The appearance of equol in plasma after ingestion of the parent compound daidzein is time-dependent on its production in the colon. Peak equol concentrations in man occur 36 h post ingestion of daidzein (Rowland et al., 2003).

To date, however, little is known about the metabolic fate of equol. So far it is not known, whether equol is a substrate for the hepatic cytochrome P450 (CYP) enzymes or not. The goal of the present study is to elucidate the phase I metabolism by using liver microsomes from Aroclor-induced male Wistar rats and from a male human. The identification of the metabolites formed was elucidated using HPLC/diode array detection, HPLC/API-ES MS, GC/EI-MS as well as reference compounds.

Methods

Chemicals

Daidzein was purchased from TCI (Tokyo, Japan). 6- and 3'-hydroxy-daidzein were from Plantech (Reading, UK). (+/-)-Equol (7,4'-dihydroxyisoflavan), 6-hydroxy-equol (6,7,4'-trihydroxyisoflavan) and 3'-hydroxy-equol (7,3',4'-trihydroxyisoflavan) were synthesized in a micro scale approach by reduction of the corresponding isoflavones (daidzein, 6-hydroxy-daidzein and 3'-hydroxy-daidzein, respectively) as described by Wessely and Prillinger (1939) and Lamberton et al. (1978). The purity of daidzein and equol was > 99% according to GC/MS analysis. $NADP^+$ (β-nicotinamide adenine dinucleotide phosphate), *N,O*-bis-(trimethylsilyl)trifluoroacetamide (BSTFA), deuterated *N,O*-bis-(trimethylsilyl)acetamide (d9-BSA) and dimethylsulfoxide were obtained from Sigma-Aldrich Chemical Co. (Taufkirchen, Germany). All other chemicals were of the highest grade available.

Preparation and characterization of rat and HLM

Microsomes were prepared and pooled from the livers of 10 Aroclor-treated male Wistar rats according to standard procedures as described by Lake (1987). Treatment with Aroclor 1254 (one intraperitoneal injection on day 1 of a dose of 500 mg/kg body weight dissolved in sesame oil at 100 mg/mL, killed on day 6) was carried out to induce hepatic CYP enzymes. HLM were a friendly gift of Prof. M. Metzler, University of Karlsruhe, Germany. They were prepared from a normal liver tissue sample of a middle-aged Caucasian man in the same way as described above. The liver sample was obtained with appropriate human use approvals. Protein concentrations were determined using Pierce bicinchoninic reagent. CYP concentrations were measured as described by Omura and Sato (1964). The rat liver microsomes were further characterized by the specific activities of major CYP

enzymes as determined by the method of Burke et al. (1994). Hepatic microsomes from Aroclor-treated rats were found to contain 1.69 nmol CYP per mg protein. 7-Ethoxycoumarin-deethylase (ECOD), 7-ethoxyresorufin-O-deethylase (EROD) and 7-pentoxyresorufin-O-dealkylase (PROD) activity was found to be 23.5, 15.1 and 0.22 nmol/mg protein/min, respectively. HLM contained 0.32 nmol CYP per mg protein.

Incubation with microsomes and extraction

Standard incubation mixtures with rat liver microsomes contained 2 mg microsomal protein, 100 nmol equol (dissolved in 40 µL DMSO) in a final volume of 2 mL 50 mM potassium phosphate buffer pH 7.4. After 2 min pre-incubation at 37°C in a shaking water bath the reaction was started by adding the NADPH-generating system (3 mM $MgCl_2$, 1 mM $NADP^+$, 8 mM D,L-isocitrate and 0.5 units isocitrate dehydrogenase) and stopped after 60 min by extraction with 4 x 2 mL ice-cold ethyl acetate. Controls were carried out by omitting the NADPH-generating system or by using heat-inactivated microsomes. The organic solvent was dried under a nitrogen stream at room temperature. The residue was dissolved in 50 µL methanol and 3950 µL water and applied to a reversed phase-18 cartridge (Waters, Eschborn, Germany). The column was first rinsed with 5 mL 20% aqueous methanol and equol and the metabolites were then eluted with 5 mL 70% aqueous methanol. The eluate was dried under nitrogen and the residues were dissolved in 200 µL aqueous 50% methanol. The samples were analyzed immediately by HPLC. All glass tubes used in this study were presilanized with 5% (v/v) dimethyldichlorosilane in toluene to avoid loss of hydroxylated equol metabolites due to adsorption to the glass surface. Incubations with HLM were carried out in the same way with the exception that the incubation mixtures contain 4 mg microsomal protein and 50 nmol equol.

HPLC analysis

HPLC separation of the oxidative metabolites was carried out on a Prontosil (250 mm x 4.6 mm i.d., particle size 3 µm) reversed-phase column (Bischoff, Leonberg, Germany). The solvent system consisted of 0.1% formic acid in water (pH = 3) (A) and acetonitrile (B) with the following linear gradient: from 15% to 35% B in 50 min, from 35% to 50% in 10 min, and from 50% to 60% in 30 min. The flow rate was 0.9 mL/min and the eluate was recorded with a diode array detector at 280 nm. Observed peaks were scanned between 190 and 400 nm.

GC/MS analysis of hydroxylated metabolites

GC/MS was carried out on a Finnigan MAT system (gas chromatograph model GCQ connected to an ion trap mass detector) (Thermo Electron Corporation, Bremen, Germany). The metabolites were isolated by HPLC and freeze-dried. For GC/MS analysis, the dry residues were derivatized with BSTFA or d9-BSA for at least two hours at room temperature. The TMS-derivatives were analyzed using a nonpolar capillary column (MDN-5S, 30 m x 0.25 mm ID, 0.25 µM film thickness, Supelco, Taufkirchen, Germany) and a linear temperature gradient (60°C for 1 min then 30°C/min to 250°C, hold for 10 min, then 1°C/min to 275°C and hold for 5 min). The injector port temperature was 50°C. Mass spectra were obtained by electron impact (EI) ionization at 70 eV and an ion source temperature of 150°C. Full scan spectra (mass range 50 - 750 amu) were recorded at rate of 2 spectra per second. Furthermore, the selected ion mode (SIM) was used for the detection of equol and its metabolites.

HPLC/MS analysis

HPLC/MS analysis was performed on an HP 1100 series HPLC (Agilent Technologies, Waldbronn, Germany) equipped with an autoinjector, quaternary HPLC pump, column heater, UV detector and HP Chem Station for data collection and

handling. The HPLC was interfaced to an HP series 1100 mass selective detector equipped with an API-ES chamber. For the analysis of oxidative metabolites conditions in the positive mode were as follows: capillary voltage 4 kV; fragmentor voltage 80 V; nebulizing pressure 50 psi; drying gas temperature 350°C; drying gas flow 10 L/min. Data were collected using both the scan mode and SIM mode. Spectra were scanned over a mass range of m/z 100 - 500 at 1.03 s/cycle.

Results

Formation and separation of rat microsomal metabolites of equol

Equol (figure 1) was incubated with hepatic microsomes of Aroclor-treated male Wistar rats. Aroclor 1254 induces CYP enzymes, especially of the 1A but also of the 2B subfamily (Burke et al., 1985; Correia, 1995). Therefore, the use of Aroclor-induced microsomes increases both the variety of the metabolites formed and their yield, thus facilitating the elucidation of the structures.

The complete organic extract of each incubation was analyzed by reversed phase HPLC with diode array detection. Equol was extensively metabolized. Eleven metabolites were clearly detectable by HPLC analysis (figure 2). These products were not observed when NADPH was omitted or heat-inactivated microsomes were used.

Furthermore, the extracted metabolites were analyzed by HPLC/MS with positive API-ES and by GC/EI-MS after trimethylsilylation. The mass spectra indicated the formation of seven mono- and four dihydroxylated metabolites. For the correlation of HPLC and GC peaks, each HPLC peak was isolated and analyzed by GC/MS after derivatization. The chromatographic and MS data, the UV maxima as well as the assigned chemical structures and the percentage of total metabolite formed are summarized in table 1.

Approach for the elucidation of metabolite structures

Use of reference compounds

6-Hydroxy-equol and 3'-hydroxy-equol were synthesized in a micro scale approach (see Material and Methods) and employed as reference compounds for co-chromatography and comparison with mass spectra. These standards proved to be helpful tools for the identification of equol metabolites. E.g., equol metabolites which are also generated in the microsomal metabolism of 3'-hydroxy-equol must contain an additional hydroxyl group in position C-3' of the B-ring.

DMD Fast Forward. Published on September 30, 2005 as DOI: 10.1124/dmd.105.004929
This article has not been copyedited and formatted. The final version may differ from this version.

HPLC/MS and GC/MS analysis

Mass spectrometry can be used to determine the molecular weight of the metabolites and to clarify the distribution of hydroxyl groups between the A- and the B-ring of the isoflavan molecule. GC/MS with EI ionization (70 eV) of trimethylsilylated (TMS) derivatives of the metabolites gave in most of the cases mass spectra with an intense molecular ion or [M^+ - 15] ion (loss of a CH_3 radical) as demonstrated in figure 3. EI mass spectra can thus be used to determine the molecular weight of the metabolites. Furthermore, in contrast to genistein and daidzein equol showed a distinct fragmentation pattern using EI ionization. To minimize the uncertainty in the interpretation of the mass spectra we used BSTFA as well as d9-BSA for the derivatization. With BSTFA every proton in the hydroxyl groups is substituted by a trimethylsilyl group (TMS; m/z = 73), while per-deuterated TMS groups (d9-TMS; m/z = 82) are formed when using d9-BSA. By comparison of the mass spectra of the derivatives, information about the number of hydroxyl groups in the molecule and about the structure of the formed fragments is obtained. Figure 3 shows the EI mass spectra of equol, 3'-hydroxy-equol and 6-hydroxy-equol after derivatization with BSTFA and d9-BSA. In figure 4 the proposed fragmentation pathway of the TMS derivative of equol is depicted. Important fragments are formed via retro Diels-Alder (rDA) reaction in the C-ring. The molecule is fragmented into a dien- (**a**) and an en- (**b**) component. It depends on the molecule which component is the main product. E.g. for equol and 3'-hydroxy-equol the en-component is formed more exclusively (m/z 192 and 280, respectively) while in the case of 6-hydroxy-equol the en- and the dien-component are formed to the same extent (m/z 192 and 282) (figure 3). Furthermore, it must be taken into account that the dien-component **a** might react to **c** by migration of the TMS group to the keto group. The rDA-fragments provide important information about the degree of the substitution at each phenolic ring.

Besides the rDA-reaction further fragmentation is observed in the C-ring. The fragment at m/z 206 in the mass spectrum of equol is assigned to be the alkene ionic radical **d,** which is stabilized by the +I-effect of the methyl and phenyl groups (see figure 4). Mass spectra of A-ring substituted equol derivatives show a fragment ion at m/z 295, which is proposed to occur via the fragmentation pathway shown in figure 5.

Valuable information about the location of the hydroxyl groups can also be obtained by HPLC/MS with positive API-ES if a relatively low fragmentor voltage of 80 V is used (see Material and Methods). A higher fragmentor voltage leads to the complete breakdown of the molecule. In figure 6 the fragmentation pathway of equol and aromatic hydroxylated equol-derivatives is depicted. The fragmentation pattern can be used to determine the number of hydroxy groups in the A- or the B-ring. The loss of a hydroxystyrene derivative result in the ionic dien component α, which gives information about the hydroxylation degree in the A-ring. The loss of a hydroxyphenol derivative leads to the fragment β, which gives information about the number of hydroxyl groups in the B-ring.

Theoretical considerations about the stereochemistry of aliphatic hydroxylated metabolites

Possible positions for the aromatic hydroxylation of equol by CYP enzymes are the positions C-8 and C-6 in the A-ring as well as C-3' (equivalent to C-5') in the B-ring. Possible positions for the aliphatic hydroxylation are C-2, C-3 and C-4 in the C-ring.

In contrast to genistein and daidzein equol possesses a chiral center at C-3 in the C-ring. The synthesis of equol results in the mixture of the two enantiomers, R-(+)- and S-(-)-equol (Lamberton et al., 1978). With respect to the hydroxylation at the aromatic positions C-6, C-8 and C-3' as well as at the aliphatic position C-3, the corresponding R- and S- enantiomers are formed. Hydroxylation at the aliphatic

positions C-2 and C-4 leads to the formation of a second asymmetric center in the C-ring and four stereoisomers can theoretically be formed. Figure 7 depicts the four possible stereoisomers of 4-hydroxy-equol. In analogy, the corresponding products can be postulated after introduction of a hydroxyl group at C-2.

Identification of microsomal metabolites of equol after incubation with Aroclor-induced rat liver microsomes

A representative HPLC profile of the microsomal metabolites of equol is depicted in figure 2.

The GC/MS analysis of the TMS derivative of the major microsomal metabolite (peak **11**, figure 2) shows a molecular ion at m/z 474 and a fragment ion m/z 280 indicating a mono-hydroxylated equol structure with two hydroxyl groups in the B-ring. The positive HPLC/API-ES mass spectrum displays a quasi-molecular ion $[M + 1]^+$ at m/z 256, indicating a mono-hydroxylation, and a diagnostic fragment ion at m/z 123, implying an unchanged A-Ring. Furthermore, metabolite **11** co-elutes with the synthesized reference compound 3'-hydroxy-equol. Taken together, metabolite **11** can be identified as 3'-hydroxy-equol. It is the main product of the microsomal metabolism of equol and accounts for up to 60% calculated on the basis of the peak area at λ = 280 nm.

Peak **10** was identified by co-chromatography in GC/MS with the synthesized reference compound as 6-hydroxy-equol. The positive API-ES mass spectrum displays a quasi-molecular ion $[M + 1]^+$ at m/z 256 - which confirms the mono-hydroxylation - and a diagnostic fragment ion at m/z 139 implying a hydroxylated A-ring (figure 6).

Metabolite **9** represents an A-ring mono-hydroxylated isoflavan according to its mass spectral data (table 1). The EI and API-ES mass spectra are found to have the same

fragment ions as 6-hydroxy-equol (metabolite **10**), which has already been identified. The spectra of these two metabolites only differ in the intensities of the fragment ions. Remaining possible positions for the introduction of an additional hydroxyl group in the A-ring are C-5 and C-8. Hydroxylation at C-5 would mean a hydroxylation in the meta position relative to the existing hydroxy group at C-7, which is very unusual and is to our knowledge so far not described. Therefore, we assign peak **9** to be 8-hydroxy-equol.

Peaks **4, 5**, **6** and **8** show molecular ions at m/z 474 implying the introduction of one additional hydroxyl group. The EI mass spectra of these metabolites exhibit $[M - 90]^+$ ions at m/z 384 suggesting the introduction of one additional double bond into the equol molecule. The double bond is derived by the elimination of a trimethylsilylated aliphatic hydroxyl group during GC/MS analysis. Hydroxylation in the aliphatic position of equol can generally be recognized by the loss of a TMSOH-group $[M - 90]^+$. Thus it is assumed that HPLC peaks **4**, **5**, **6** and **8** represent aliphatic mono-hydroxylated metabolites of equol. Possible positions of equol for the aliphatic hydroxylation are C-2, C-3 and C-4 at the C-ring.

The GC mass spectrum of the TMS derivatives of metabolite **4** lacks the ions m/z 192 and 177, respectively, or 179, which are minor fragments of all other metabolites and are derived by the formation of the en-component or a hydroxybenzylium ion (m/z 179). Furthermore, peak **4** additionally exhibits strong fragment ions at m/z 280 and m/z 268, which are formed by the introduction of a hydroxyl group at C-3. On the basis of these data, peak **4** is assigned to be 3-hydroxy-equol. Figure 3 shows the EI mass spectra after derivatization with BSTFA and d9-BSA; figure 8 the proposed fragmentation pathway.

Examination of the isolated peaks **5** and **8** shows identical results in the GC/MS:

Each peak was separated into two products, which differed in the retention times (16.20 and 17.12 min), but showed the same mass spectra with molecular ions at m/z 474 (table 1). These metabolites can be tentatively identified as the stereoisomers of 4-hydroxy-equol. The EI mass spectra after derivatization with BSTFA and d9-BSA and the corresponding fragmentation pathways are depicted in figures 11 and 12. The EI mass spectra of these metabolites exhibit $[M - 90]^+$ ions at m/z 384 suggesting a hydroxylation in an aliphatic position due to the loss of a TMSOH-group. For the formation of the basic ion at m/z 267 and the fragment ions at m/z 282 and 355 we suggest the fragmentation pathway depicted in figure 10. Hydroxylation in the aliphatic positions C-4 in the C-ring of the (+/-)-equol molecule leads to the insertion of an additional asymmetric C-atom and, therefore, to the formation of four stereoisomers as shown in figure 7. The four possible stereoisomers were separated into two diastereomeric pairs (e.g. 3S,4R and 3S,4S separated from 3R,4S and 3R,4R) under the used conditions for liquid chromatography. These pairs then were separated into the corresponding diastereomers by GC/MS analysis. Since no chiral column material was used, the two corresponding enantiomers of peak **5** and **8** show identical retention times in the GC/MS. The mass spectra were identical to those published by Joannou et al. (1995) and Heinonen et al. (1999), who identified the metabolites as the diastereomeric forms *cis*- and *trans*-4-hydroxy-equol.

For peak **6**, the third aliphatic hydroxylated metabolite, we found a complex fragmentation pattern in the EI mass spectrum since this metabolite is rather unstable. The most intense ion in the EI mass spectrum is not the molecular ion (m/z 474 only 5%) but m/z 402, which can be derived by the loss of a TMS-group. In contrast, the API-ES mass spectrum allows an unambiguous interpretation: It shows a quasi-molecular ion $[M + 1]^+$ at m/z 259 (figure 11) implying a mono-hydroxylated derivative. Further fragment ions are m/z 241 and 231, which are derived by the loss

of H_2O and CO, respectively. The most intense ion is m/z 137, which can be explained by the formation of the ionic 3-phenylethanal **a**. This product can further be degraded to **b**. In figure 12 the proposed fragmentation pathway is shown. On the basis of these findings, peak **6** is tentatively identified as 2-hydroxy-equol. Nonetheless, the final allocation of the structure requires further spectroscopic information or reference compounds. From a theoretical point of view, the formation of four stereoisomers - as shown for 4-hydroxy-equol - is possible. However, with the analytical methods used we got no indication of further stereoisomeric 2-hydroxy-equol derivatives.

Peak **7** is formed in the microsomal metabolism of equol and 3'-hydroxy-equol. In the EI mass spectrum a molecular ion at m/z 562 is observed as well as a quasi-molecular ion $[M + 1]^+$ at m/z 287 in the API-ES mass spectrum. It is concluded that metabolite **7** is a mono-hydroxylated 3'-hydroxy-equol derivative. Based on the EI and API-ES mass spectra a dihydroxylated A-ring derivative is likely. Since the metabolite does not co-elute with 6,3'-dihydroxy-equol (a metabolite which is formed during incubation of 3'-hydroxy-equol with the enzyme tyrosinase, data not shown) we preliminary assign peak **7** to be 8,3'-dihydroxy-equol.

Metabolites **1, 2** and **3** are formed only in small yields. According to the API-ES mass spectra they correspond to dihydroxylated equol derivatives. The isolated HPLC peaks -degraded during GC/MS analysis. Therefore, the structures have not yet been identified. These three metabolites are also formed in the microsomal metabolism of 3'-hydroxy-equol, implying that peak **1, 2** and **3** are mono-hydroxylated 3'-hydroxy-equol derivatives.

Human microsomal metabolites of equol

HLM have been used to gain information about the metabolites formed in vitro by humans in comparison to the rat. Equol is converted to six metabolites by HLM. Main

metabolites are the aromatic mono-hydroxylated products 3‘- and 6-hydroxy-equol. Further metabolites are 8-hydroxy-equol and both diastereomeric pairs of 4-hydroxy-equol (figure 13). In trace amounts two monohydroxylated 3’-hydroxy-equol derivatives are found.

Discussion

In the present study, we have investigated the in vitro phase I metabolism of equol using pooled Aroclor-induced rat liver microsomes. Eleven metabolites were formed, separated by HPLC and GC and identified with the help of their HPLC/API-ES and GC/EI-MS spectra and by comparison with reference compounds. Our results clearly indicate that equol is a substrate for CYP enzymes. A scheme of the identified metabolites is shown in figure 14. Preliminary experiments with HLM from one male individual suggest that the oxidative metabolism of equol may also be relevant to humans although HLM caused in our experiments - compared to the Aroclor-induced rat liver microsomes - a less complex metabolite profile. This is not very surprising since Aroclor 1254 induces a variety of different CYP enzymes including also CYP enzymes which are usually not expressed in the liver e.g. CYP 1A1. Furthermore the amount of CYP enzyme per nmol equol substrate was higher in incubation mixtures with rat liver microsomes. However, in both cases, the rat and the human microsomal metabolism, 3'-hydroxy-equol as well as 6- and 8-hydroxy-equol and the aliphatic hydroxylated metabolite 4-hydroxy-equol are the main products. Further studies with pooled HLM or with a larger number of different HLM as well as with human recombinant CYP enzymes are needed to get additional information on the interindividual variation of the metabolite pattern in humans and on the CYP enzymes involved in the formation of the different metabolites.

4-hydroxy-equol has already been identified by Kelly at al. (1993), Joannou et al. (1995) and Heinonen et al. (1999) in urine of human volunteers after the consumption of soy. The in vivo formation of 4-hydroxy-equol is proposed to occur via the reductive metabolism of daidzein to dihydrodaidzein and a further reduction step of the keto group in the C-ring of dihydrodaidzein to 4-hydroxy-equol (figure 1).

DMD Fast Forward. Published on September 30, 2005 as DOI: 10.1124/dmd.105.004929
This article has not been copyedited and formatted. The final version may differ from this version.

Our in vitro experiments with rat liver microsomes and HLM show that the formation of 4-hydroxy-equol can also occur via hydroxylation of equol by CYP enzymes. Maybe both pathways are relevant for the in vivo situation. The same may hold for the aromatic hydroxylated equol derivatives formed by human and rat liver microsomes. Kulling et al. (2000 and 2001) have been able to show that the soy isoflavones daidzein and genistein are good substrates for CYP enzymes in vitro. Furthermore, several mono- and dihydroxylated daidzein and genistein as well as mono-hydroxylated equol metabolites have been identified in vivo (Kulling et al., 2001; Heinonen et al., 2003). Therefore, the formation of the aromatic hydroxylated equol metabolites may occur via reduction of the corresponding hydroxylated isoflavones or via hydroxylation of equol by CYP450 enzymes as shown in this study. Further studies are needed to clarify the importance of these two metabolic pathways. It seems to be likely that both pathways are of relevance for the in vivo formation of the hydroxylated equol metabolites. Therefore, our findings might have a substantial impact on the understanding of the biotransformation of isoflavones.

Joannou et al. and Kelly et al. tentatively identified the detected derivatives of 4-hydroxy-equol in human urine as *cis*- and *trans*-form based on mass spectrometric data and micro scale synthesis of possible reference compounds, whose structure were characterized by GC/MS (Kelly at al., 1993; Joannou et al., 1995). However, Heinonen et al. detected only *cis*-4-hydroxy-equol. They used reference compounds fully characterized by 2D ^{1}H and ^{13}C NMR as well as molecular mechanical calculations (Heinonen et al., 1999; Wahala et al., 1997). Therefore, it seems likely that in vivo only *cis*-4-hydroxy-equol is formed. Hydroxylation of racemic (+/-)-equol with human and rat liver microsomes leads to the formation of all four possible stereoisomers of 4-hydroxy-equol, the *cis*-isomers 3S,4R- and 3R,4S-4-hydroxy-equol as well as the *trans*-isomers 3S,4S- and 3R,4R-4hydroxy-equol (figure 7). *Cis*-

4-hydroxy-equol - the intermediate metabolite in the intestinal bacterial metabolism of daidzein to S-(-)-equol as identified by Heinonen et al. (1999) - has to be 3S,4R-4-hydroxy-equol. Probably, 3S,4R-4-hydroxy-equol is formed by CYP enzymes in vivo as well (figure 15).

The hydroxylated metabolites exert interesting biological properties: The anticancer activities of both 4-hydroxy-equol isomers have been studied by Wahala et al. (1997). Both isomers inhibit the growth of prostate cells (LNCaP 90) much more effectively than the parent compound daidzein. The activities were comparable to that of genistein; however, *cis*- and *trans*-4-hydroxy-equol were less cytotoxic. Regarding the antioxidant activity it has been shown that equol is more potent than genistein or daidzein and that the hydroxylated metabolites of genistein and daidzein exert an even higher antioxidant efficacy than equol (Arora et al., 1998; Rimbach et al., 2003; Turner et al., 2004). Therefore, studies on the antioxidant capacity of the hydroxylated equol metabolites seem to be interesting. Reference compounds are needed to investigate the biological effects in detail.

In conclusion, this is the first study to show that equol is a substrate for CYP enzymes and is therefore not inevitably the metabolic end product of daidzein. It is well established that the biological activities of isoflavones are dramatically altered with the chemical structure. On the basis of these findings, it can be assumed that the hydroxylated products have other biological properties than those of the parent compound. Recent studies show that the formation of equol through the action of intestinal bacteria might play a central role regarding the chemopreventive potential of isoflavones (Frankenfeld et al., 2004). Therefore it seems necessary to completely understand the metabolism pathways of isoflavones and to identify all metabolites,

which were formed during this process - even if these metabolites might appear in small quantities.

References

Arora A, Nair MG, Strasburg GM (1998) Antioxidant activities of isoflavones and their biological metabolites in a liposomal system. *Arch Biochem Biophys* **356**:133-141.

Axelson M, Kirk DN, Farrant RD Cooley G, Lawson AM, Setchell KD (1982) The identification of the weak oestrogen equol [7-hydroxy-3-(4'-hydroxyphenyl)-chroman] in human urine. *Biochem J* **201**:353-357.

Burke MD, Thompson S, Waever R, Wolf C, Mayer R (1994) Cytochrome P450 specifities of alkoxyresorufin O-dealkylation in human and rat liver. *Biochem Pharmacol* **48**:923-936.

Burke MD, Thompson S, Elcombe CR, Halpert J, Haaparanta T, Mayer RT (1985) Ethoxy-, pentoxy- and benzyloxyphenoxazones and homologues: A series of substrates to distinguish between different induced cytochrome P-450. Biochem. Pharmacol **34**: 3337-3345.

Chang YC, Nair MG (1995) Metabolism of daidzein and genistein by intestinal bacteria. *J Nat Prod* **58**:1892-1896.

Correia MA (1995) Rat and human liver cytochromes P450. In: Cytochrome 450: Structure, Mechanism, and Biochemistry (P. R. O. d. Montellano, Ed.) pp. 607-630. Plenum Press, New York.

Frankenfeld CL, McTiernan A, Aiello EJ, Thomas WK, LaCroix K, Schramm J, Schwartz SM, Holt VL, Lampe JW (2004) Mammographic density in relation to daidzein-metabolizing phenotypes in overweight, postmenopausal women. *Cancer Epidemiol Biomarkers Prev* **13**:1156-62.

Heinonen S, Wahala K, Adlercreutz H (1999) Identification of isoflavone metabolites dihydrodaidzein, dihydrogenistein, 6'-OH-O-dma, and cis-4-OH-equol in human urine

by gas chromatography-mass spectroscopy using authentic reference compounds. *Anal Biochem* **2742**:211-219.

Heinonen SM, Hoikkala A, Wahala K, Adlercreutz H (2003) Metabolism of the soy isoflavones daidzein, genistein and glycitein in human subjects. Identification of new metabolites having an intact isoflavonoid skeleton. *J Steroid Biochem Mol Biol* **87**:285-299.

Joannou GE, Kelly GE, Reeder AY, Waring M, Nelson C (1995) A urinary profile study of dietary phytoestrogens. The identification and mode of metabolism of new isoflavonoids. *J Steroid Biochem Mol Biol* **54**:167-184.

Kelly GE, Nelson C, Waring MA, Joannou GE, Reeder AY (1993) Metabolites of dietary (soya) isoflavones in human urine. *Clin Chim Acta* **223**:9-22.

Kostelac D, Rechkemmer G, Briviba K (2003) Phytoestrogens modulate binding response of estrogen receptors alpha and beta to the estrogen response element. *J Agric Food Chem* **51**:7632-7635.

Kulling SE, Honig DM, Simat TJ, Metzler M (2000) Oxidative in vitro metabolism of the soy phytoestrogens daidzein and genistein. *J Agric Food Chem* **48**:4963-4972.

Kulling SE, Honig DM, Metzler M (2001) Oxidative metabolism of the soy isoflavones daidzein and genistein in humans in vitro and in vivo. *J Agric Food Chem* **49**:3024-3033.

Lake BG (1987) Preparation and characterization of microsomal fractions for studies on xenobiotic metabolism, in: *Biochemical Toxicology* (K. Snell and B. Mullock eds), pp 138-215, IRL Press, Oxford.

Lamberton J, Suares H, Watson K (1978) Catalytic hydrogenation of isoflavones. The preparation of (+/-)-equol and related isoflavans. *Aust J Chem* **31**:455-457.

Lund TD, Munson DJ, Haldy ME, Setchell KD, Lephart ED, Handa RJ (2004) Equol is a novel anti-androgen that inhibits prostate growth and hormone feedback. *Biol Reprod* **70**:1188-1195.

Marrian GF, Haselwood GAD, Beall CXLV (1932) Equol, a new active phenol isolated from ketohydroxyestrin fraction of mare's urine. *Biochem J* **26**:1226-1232.

Morito K, Hirose T, Kinjo J, Hirakawa T, Okawa M, Nohara T, Ogawa S, Inoue S, Muramatsu M, Masamune Y (2001) Interaction of phytoestrogens with estrogen receptors alpha and beta. *Biol Pharm Bull* **24**:351-356.

Muthyala RS, Ju YH, Sheng S, Williams LD, Doerge DR, Katzenellenbogen BS, Helferich WG, Katzenellenbogen JA (2004) Equol, a natural estrogenic metabolite from soy isoflavones: convenient preparation and resolution of R- and S-equols and their differing binding and biological activity through estrogen receptors alpha and beta. *Bioorg Med Chem* **12**:1559-1567.

Omura T, Sato R (1964) The carbon monoxide-binding pigment of liver microsomes. 1. Evidence for its hemoprotein nature. *J Biol Chem* **61**:461-467.

Rimbach G, De Pascual-Teresa S, Ewins BA, Matsugo S, Uchida Y, Minihane AM, Turner R, VafeiAdou K, Weinberg PD (2003) Antioxidant and free radical scavenging activity of isoflavone metabolites. *Xenobiotica* **33**:913-925.

Rowland IR, Wiseman H, Sanders TA, Adlercreutz H, Bowey EA (2000) Interindividual variation in metabolism of soy isoflavones and lignans: influence of habitual diet on equol production by the gut microflora. *Nutr Cancer* **36**:27-32.

Rowland I, Faughnan M, Hoey L, Wahala K, Williamson G, Cassidy A (2003) Bioavailability of phyto-oestrogens. *Br J Nutr* **89**:S45-S58.

Setchell KD, Brown NM, Lydeking-Olsen E (2002) The clinical importance of the metabolite equol - a clue to the effectiveness of soy and its isoflavones. *J Nutr* **132**: 3577-3584.

Setchell KD, Clerici C, Lephart ED, Cole SJ, Heenan C, Castellani D, Wolfe BE, Nechemias-Zimmer L, Brown NM, Lund TD, Handa RJ, Heubi JE (2005) S-equol, a potent ligand for estrogen receptor beta, is the exclusive enantiomeric form of the soy isoflavone metabolite produced by human intestinal bacterial flora. *Am J Clin Nutr* **81**:1072-9.

Shutt DA, Braden AWH (1968) The significance of equol in relation to the oestrogenic responses in sheep ingesting clover with a high formononetin content. *Aust J Agric Res* **19**:545-555.

Turner R, Baron T, Wolffram S, Minihane AM, Cassidy A, Rimbach G, Weinberg PD (2004) Effect of circulating forms of soy isoflavones on the oxidation of low density lipoprotein. *Free Radic Res* **382**:209-216.

Wahala K, Koskimies JK, Mesilaakso M, Salakka AK, Leino TK, Adlercreutz H (1997) The synthesis, structure and anticancer activity of *cis*- and *trans*-4',7-dihydroxyisoflavan-4-ols. *J Org Chem* **62**:7690-7693.

Wessely F, Prillinger F (1939) Die Konstitution des Equols. *Chem Universitätslaborat Wien* **72**:629-633.

Footnotes

This work was funded by the Deutsche Forschungsgemeinschaft (grant Ku 1079/6-1).

Legends for figures

Figure 1: Intestinal bacterial metabolism of the soy isoflavone daidzein to the isoflavan equol

Figure 2: Representative HPLC chromatogram of equol metabolites formed by the incubation of equol with liver microsomes of Aroclor-induced male rats. Peak numbers refer to table 1.

Figure 3: GC/EI-MS spectra of the trimethylsilyl (TMS) and perdeuterated trimethylsilyl (d9-TMS) derivatives of equol, 3'- and 6-hydroxy-equol obtained after derivatization with BSTFA and d9-BSA. The mass shift caused by the deuterium labeling is a helpful tool for a detailed interpretation of the fragmentation pattern. Further information is given under *Results (HPLC/MS and GC/MS analysis).* A detailed explanation of the EI-MS spectra of the TMS and the d9-TMS derivative of equol is shown in figure 4.

Figure 4: Proposed fragmentation pathways of equol after trimethylsilylation with BSTFA (a) and d9-BSA (b). The percentage of the fragment ion formed is given in parentheses.

Figure 5: Conceivable formation pathway of the fragment ion *m/z* 295, which is observed in A-ring hydroxylated equol-derivatives. The m/z values of the TMS-derivative of 6-hydroxy-equol (a) and the corresponding d9-TMS derivative (b) are given.

Figure 6: HPLC/API-ES MS fragmentation pattern of hydroxylated isoflavans. The fragment ions m/z 123 and 139 give an indication to the number of hydroxyl groups at the A-ring (fragment α), and the fragment ions m/z

133 and 149 to the number of hydroxyl groups in the B-ring (fragment β).

Figure 7: The four possible stereoisomers of 4-hydroxy-equol. 4-hydroxy-equol possesses two chiral centers (C-3 and C-4).

Figure 8: Proposed fragmentation pathway of 3-hydroxy-equol.
a) TMS-derivative, b) d9-TMS-derivative

Figure 9: GC/EI-MS spectra of 4-hydroxy-equol after trimethylsilylation with BSTFA (A) and d9-BSA (B). An explanation of the mass fragmentation pattern is given in figure 10 and is described in detail under *Results.*

Figure 10: Proposed fragmentation pathway of 4-hydroxy-equol.
a) TMS-derivative, b) d9-TMS-derivative

Figure 11: HPLC/API-ES mass spectrum of metabolite 6. The most intense ion at m/z 137 (base peak) is based on the formation of an ionic 3-phenylethanal as shown in figure 12.

Figure 12: Proposed fragmentation pathway of metabolite 6, identified as 2-hydroxy-equol according to the fragment ions derived by HPLC/API-ES MS analysis. The mass fragmentation spectrum is shown in figure 11.

Figure 13: GC selected ion chromatogram of the incubation of equol with HLM. *4-hydroxy-equol is overlapped by an unknown compound having the same retention time.

Figure 14: Microsomal metabolites of equol (racemate) formed through aromatic and aliphatic hydroxylation catalyzed by CYP enzymes. Refer to table 1 for the percentages formed of each metabolite under the incubation conditions used in this study. In the case of 2- and 4-hydroxy-equol four

possible stereoisomers can be formed due to the introduction of an additional chiral center at C-2 and C-4, respectively (see figure 7).

Figure 15: Proposed stereospecific formation of 4-hydroxy-equol. Daidzein is exclusively converted to the S-(-)-equol enantiomer by the gut microflora (Setchell et al., 2005). We assume that cis-4-hydroxy-equol, described as the intermediate metabolite in the gut bacterial metabolism can also be formed via hydroxylation catalyzed by CYP enzymes. For further explanation see *Discussion*.

DMD Fast Forward. Published on September 30, 2005 as DOI: 10.1124/dmd.105.004929
This article has not been copyedited and formatted. The final version may differ from this version.

Table 1: Chromatographic and spectroscopic data as well as the proposed chemical structures of the metabolites of equol formed by liver microsomes of Aroclor-induced male Wistar rats. The percentage of total metabolite formed under the incubation conditions used in this study was calculated on the basis of the HPLC peak area at 280 nm. The base peak in the GC/EI mass spectra of the trimethylsilylated metabolites is underlined. In case of metabolites 1, 2 and 6 the molecular ion was not detected. The HPLC peak numbers correspond to HPLC chromatogram shown in figure 2.

HPLC-peak	RT in HPLC [min]	UV maxima [nm]	% of total metabolite formed	$[M + 1]^+$ HPLC/MS	RT in GC [min]	M^+, GC/MS TMS-derivative	proposed chemical structure
1	17.5	231, 284	1.3	275	18.4	490	3'-hydroxy-equol + 1 OH group
2	19.1	239,288	1.3	(275), 257	degradation; several peaks		3'-hydroxy-equol + 1 OH group
3	23.8	233, 290, 304	1.0	275	21.0	562, 368	3'-hydroxy-equol + 1 OH group
					21.1	490	
4	26.7	225,280	14.5	259	17.0	474, 280	3-hydroxy-equol
5	30.0	223, 279	5.3	241	16.2 / 17.1	474, 267	4-hydroxy-equol
6	34.2	226,286, 305	6.5	259	16.2	444	2-hydroxy-equol
					16.4	402, 179	
7	34.7	281	2.8	-	22.2	562, 268	8,3'-dihydroxy-equol
8	35.4	224, 278	0.9	241	16.2 / 17.1	474, 267	4-hydroxy-equol
9	47.6	275	3.7	259	18.4	474, 267	8-hydroxy-equol
10	48.7	222, 296	3.4	257	20.3	474	6-hydroxy-equol
11	54.2	283	59.4	259	19.2	474, 280	3'-hydroxy-equol
12	63.0	223, 282	-	243	15.3	386, 192	equol

Figure 1

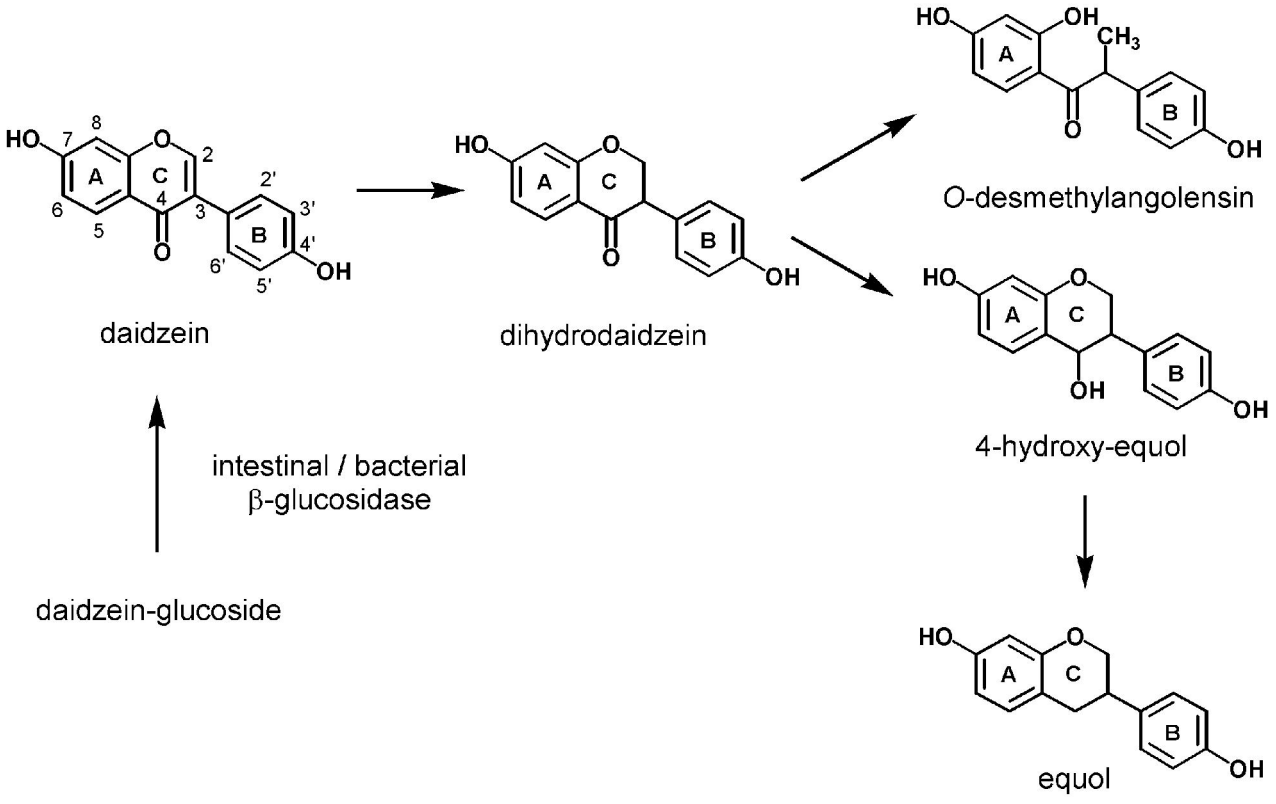
daidzein
dihydrodaidzein
O-desmethylangolensin
4-hydroxy-equol
equol
intestinal / bacterial
β-glucosidase
daidzein-glucoside

Figure 2

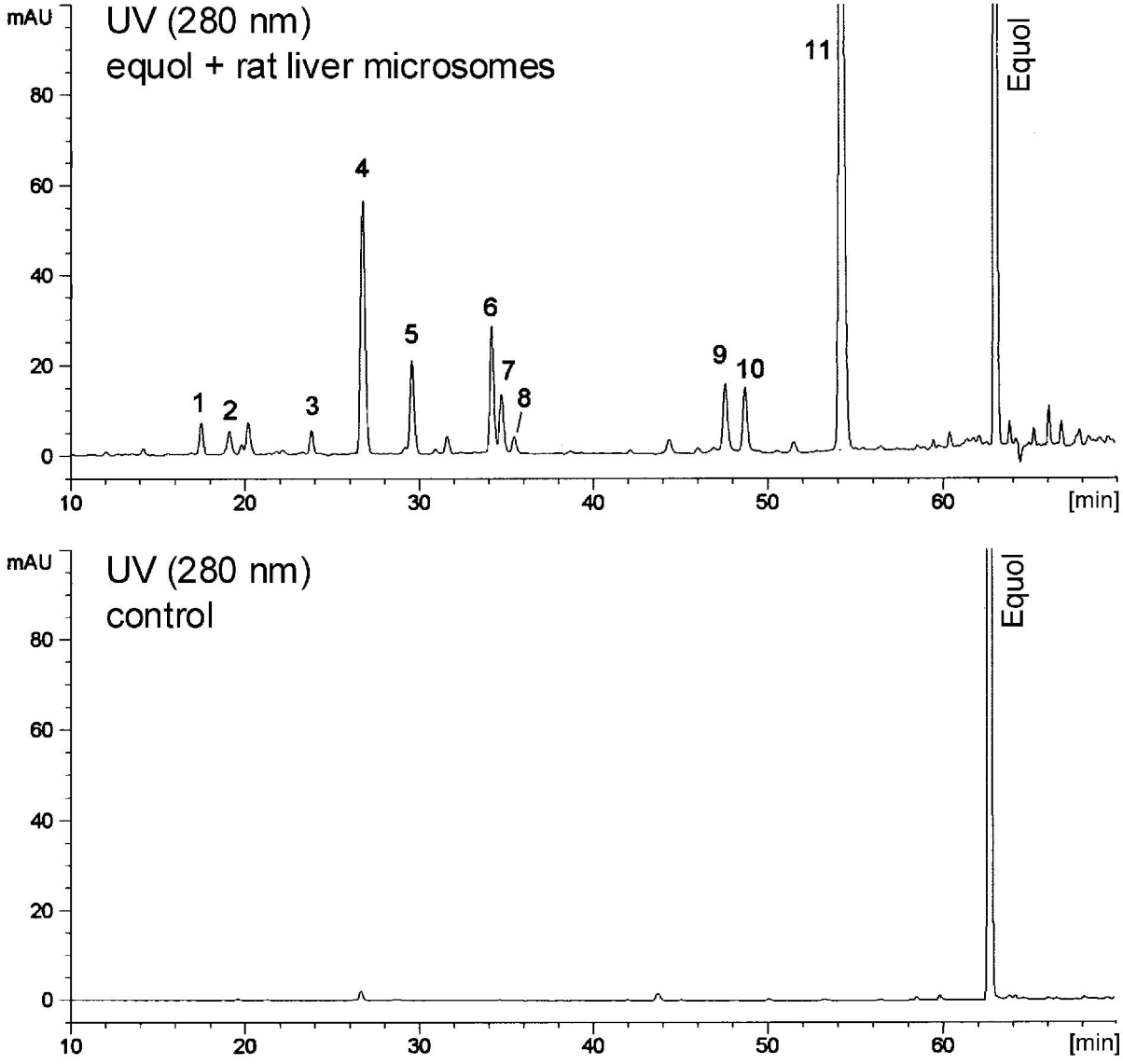
mAU
UV (280 nm)
equol + rat liver microsomes
1
2
3
4
5
6
7
8
9
10
11
Equol
0
20
40
60
80
10
20
30
40
50
60
[min]
mAU
UV (280 nm)
control
Equol
0
20
40
60
80
10
20
30
40
50
60
[min]

Figure 3

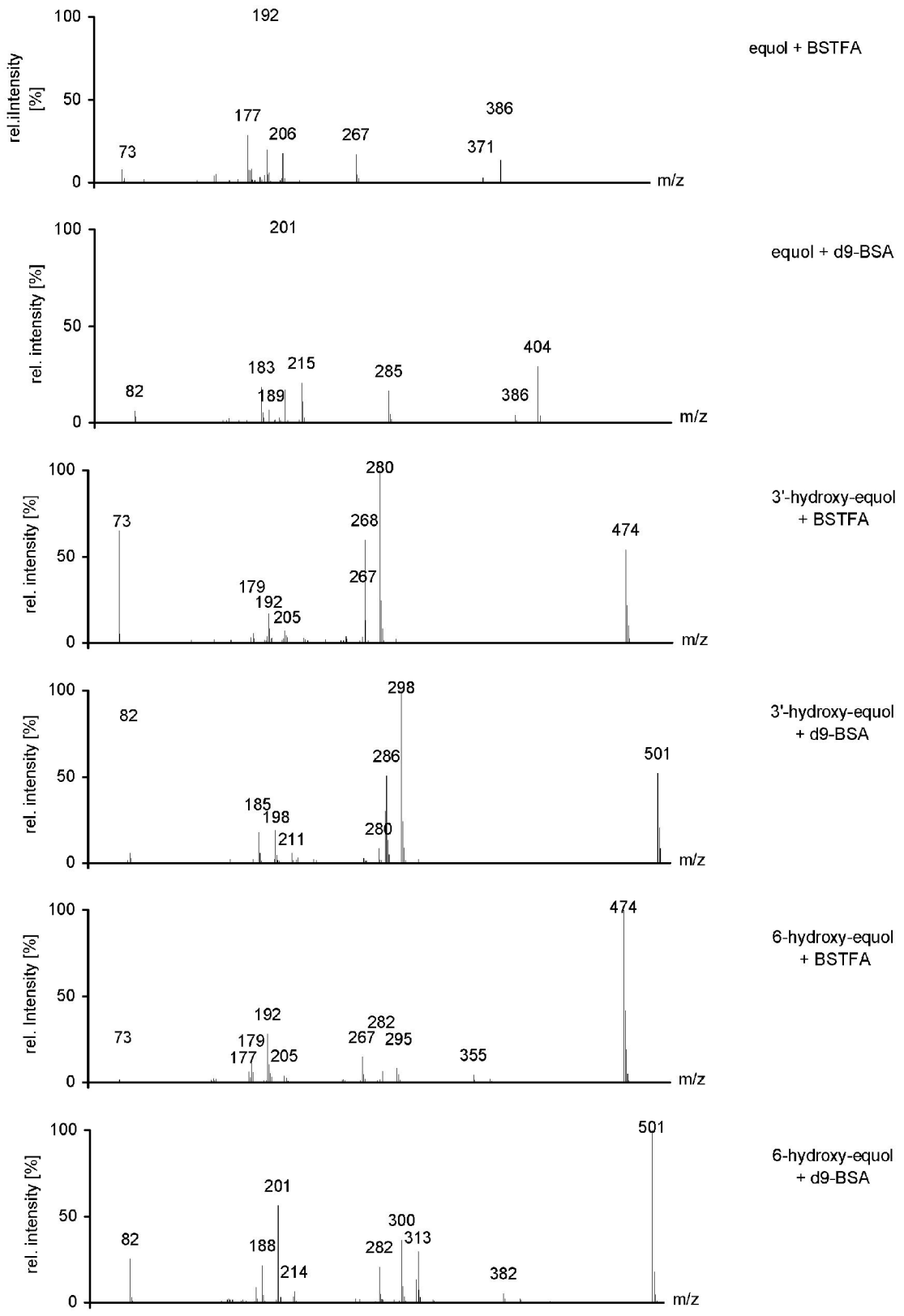
rel.iIntensity [%]
100
50
0
192
177
206
267
73
386
371
m/z
equol + BSTFA
rel. intensity [%]
201
183
215
285
82
189
404
386
equol + d9-BSA
280
73
268
474
267
179
192
205
3'-hydroxy-equol + BSTFA
298
82
286
501
185
198
211
280
3'-hydroxy-equol + d9-BSA
rel. Intensity [%]
474
192
282
73
179
267
295
177
205
355
6-hydroxy-equol + BSTFA
501
201
300
313
82
188
282
214
382
6-hydroxy-equol + d9-BSA

Figure 4

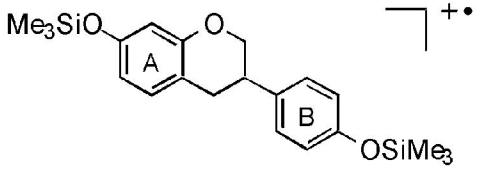

a) m/z 386 (33%)
b) m/z 404 (29%)

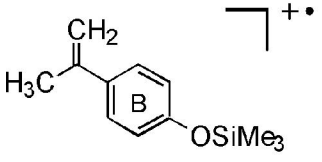

d

a) m/z 206 (18%)
b) m/z 215 (21%)

rDA

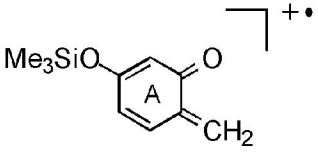

a

a) m/z 194 (5%)
b) m/z 203 (5%)

or

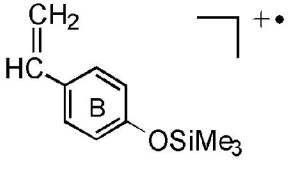

b

a) m/z 192 (100%)
b) m/z 201 (100%)

+ • SiMe3

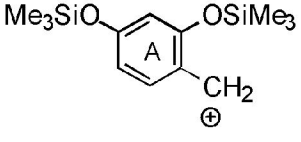

c

a) m/z 267 (19%)
b) m/z 285 (16%)

- • CH3

a) m/z 177 (29%)
b) m/z 183 (19%)

Figure 5

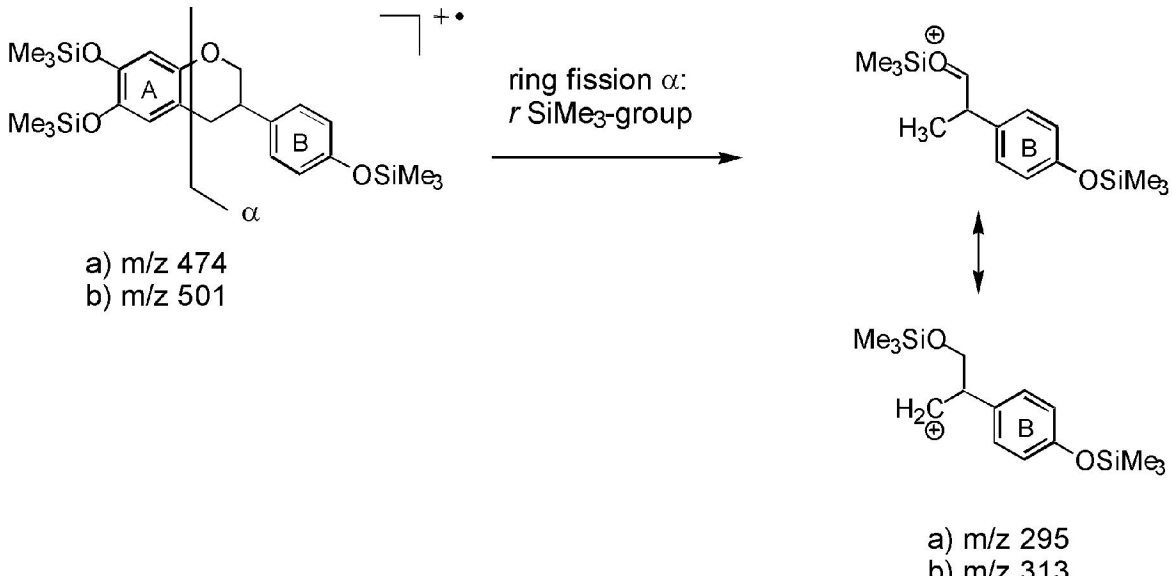

a) m/z 474
b) m/z 501

a) m/z 295
b) m/z 313

Figure 6

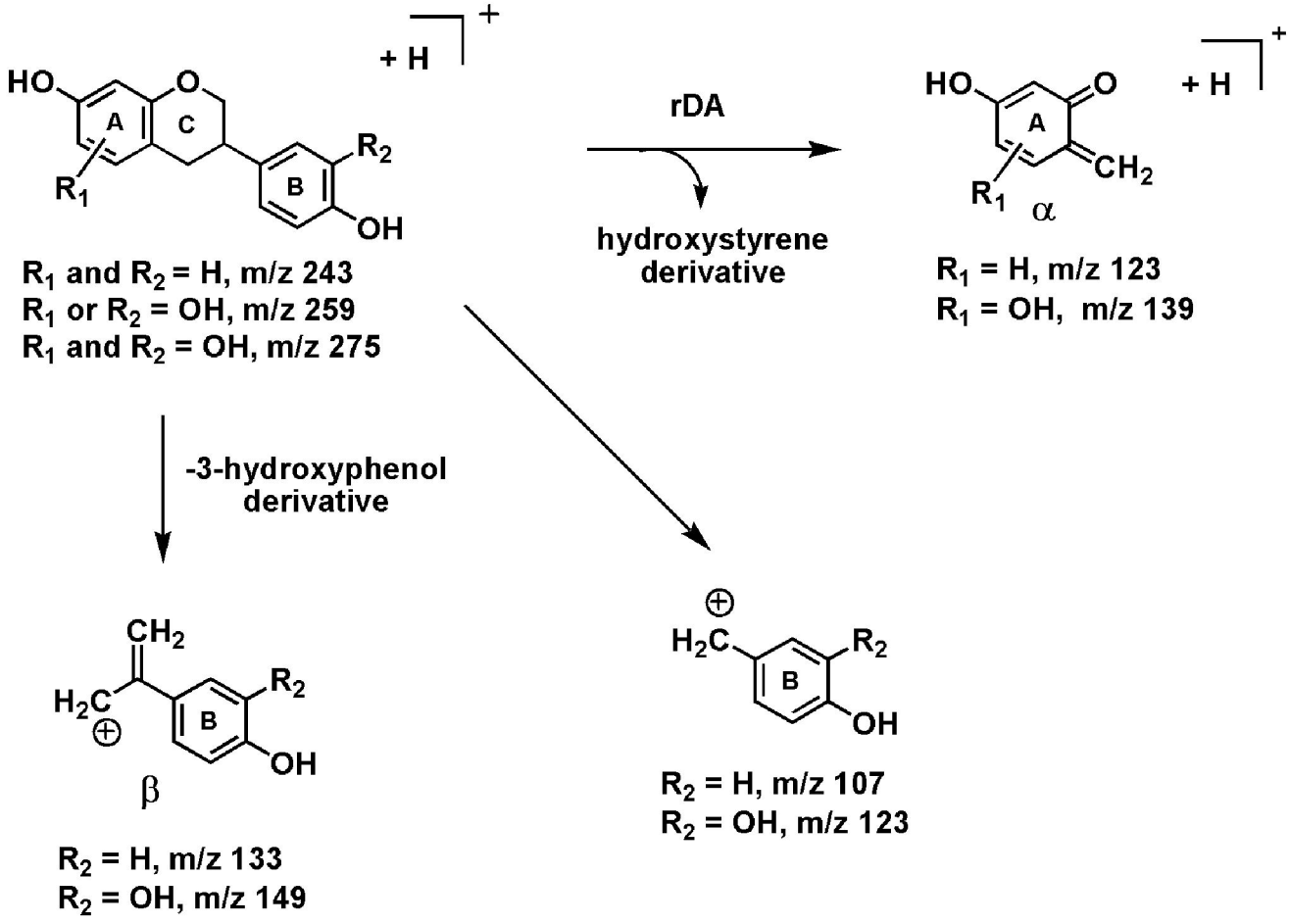
+ H
HO
O
A
C
B
R2
R1
OH
rDA
hydroxystyrene
derivative
HO
O
A
CH2
R1
α
+ H
R1 and R2 = H, m/z 243
R1 or R2 = OH, m/z 259
R1 and R2 = OH, m/z 275
R1 = H, m/z 123
R1 = OH, m/z 139
-3-hydroxyphenol
derivative
CH2
H2C
B
R2
OH
β
H2C
B
R2
OH
R2 = H, m/z 133
R2 = OH, m/z 149
R2 = H, m/z 107
R2 = OH, m/z 123

Figure 7

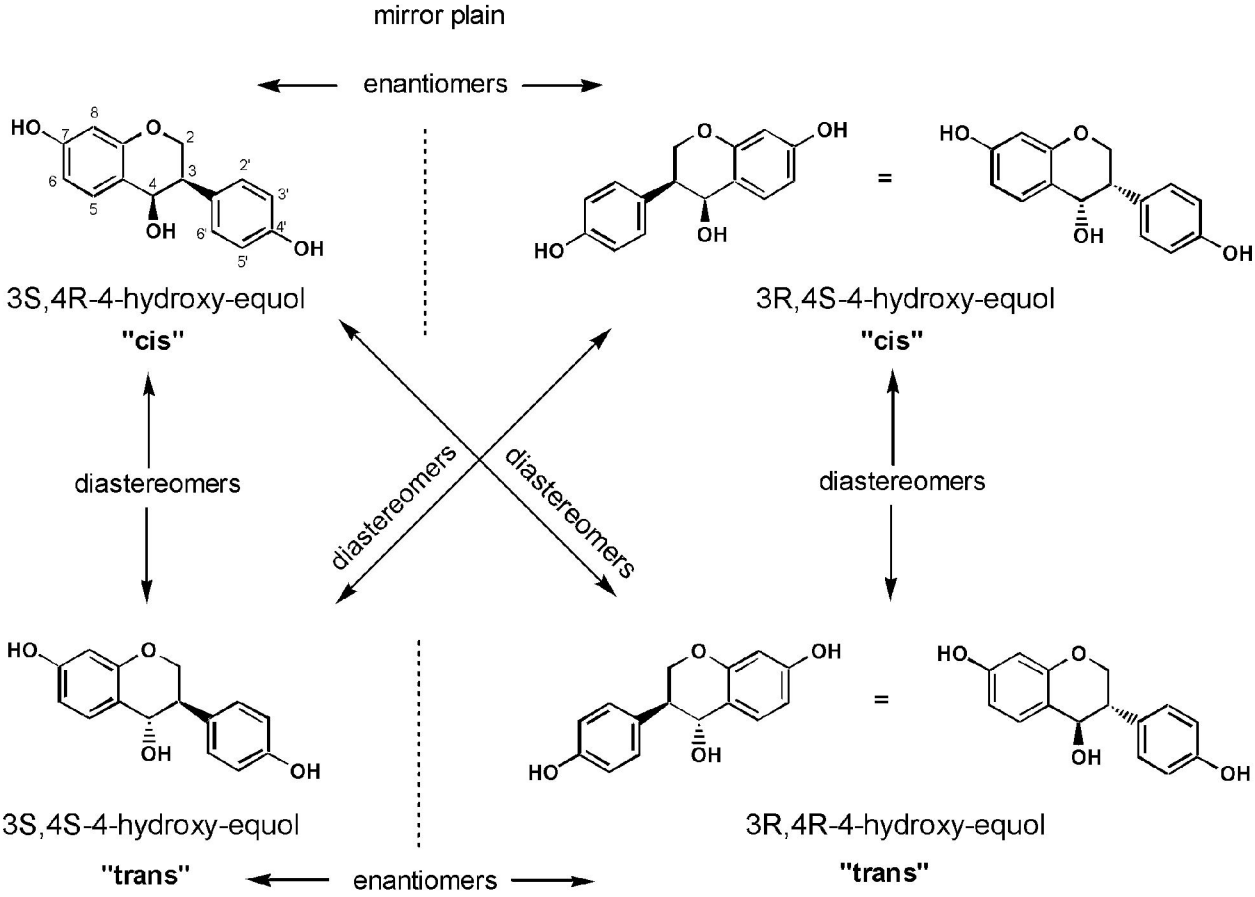
mirror plain
enantiomers
3S,4R-4-hydroxy-equol
"cis"
3R,4S-4-hydroxy-equol
"cis"
diastereomers
diastereomers
diastereomers
diastereomers
3S,4S-4-hydroxy-equol
"trans"
3R,4R-4-hydroxy-equol
"trans"
enantiomers

Figure 8

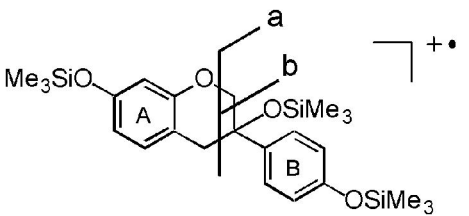

a) m/z 474
b) m/z 501

- TMSOH

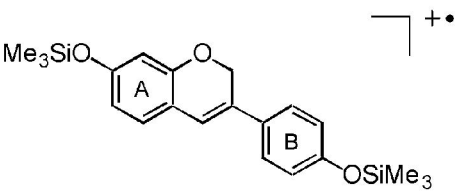

a) m/z 384
b) m/z 402

ring fission a

ring fission b

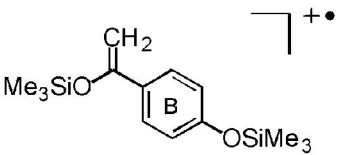

a) m/z 280
b) m/z 298

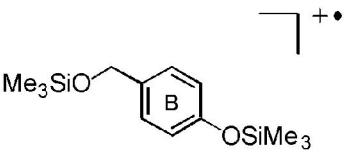

a) m/z 268
b) m/z 286

Figure 9

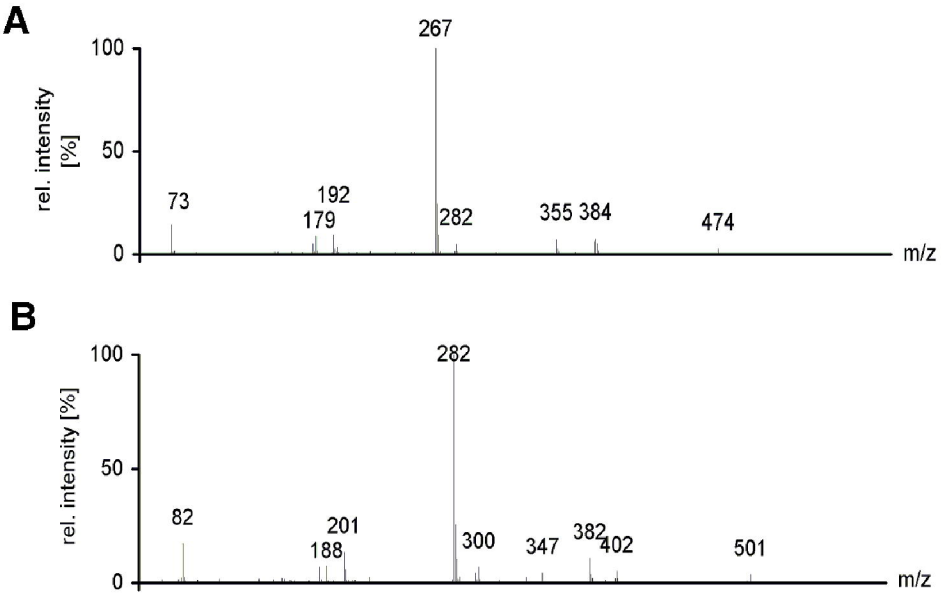
A
100
50
0
rel. intensity [%]
267
73
192
179
282
355 384
474
m/z
B
100
50
0
rel. intensity [%]
282
82
201
188
300
347
382
402
501
m/z

Figure 10

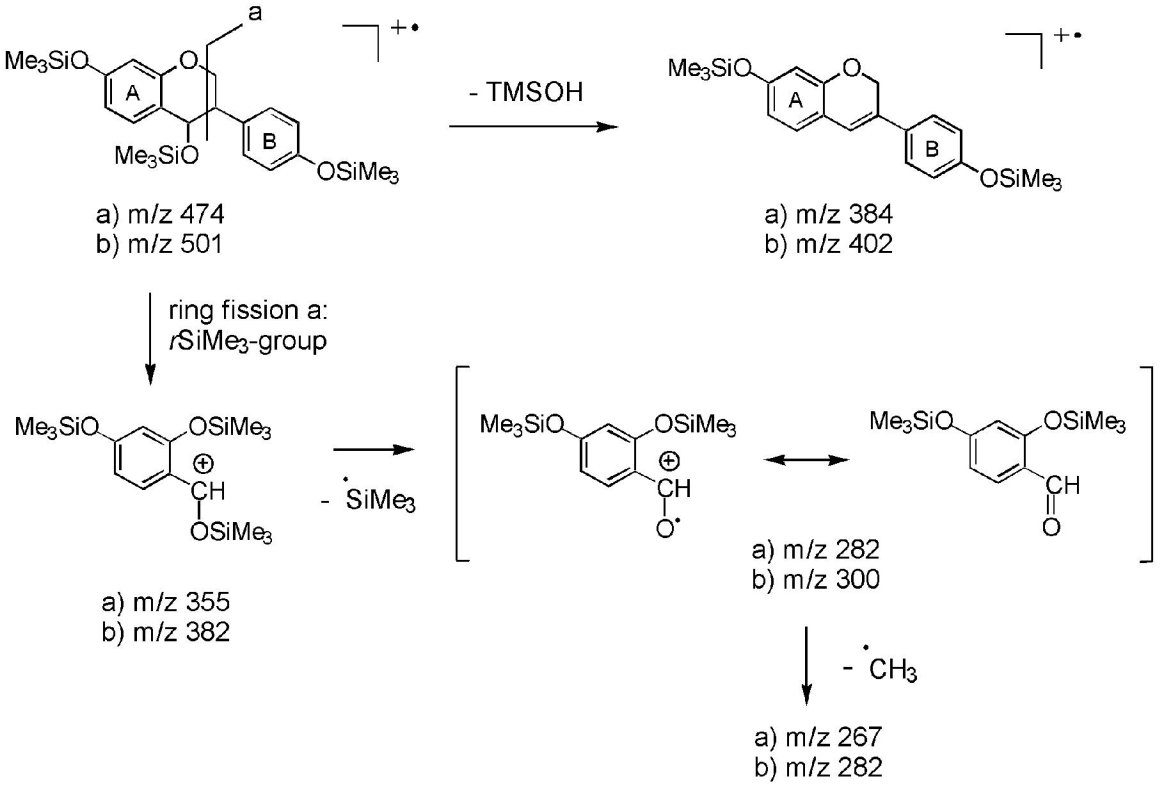
a
Me3SiO
A
B
Me3SiO
OSiMe3
+•
- TMSOH
a) m/z 474
b) m/z 501
a) m/z 384
b) m/z 402
ring fission a:
rSiMe3-group
OSiMe3
CH
- •SiMe3
a) m/z 355
b) m/z 382
O•
a) m/z 282
b) m/z 300
- •CH3
a) m/z 267
b) m/z 282

Figure 11

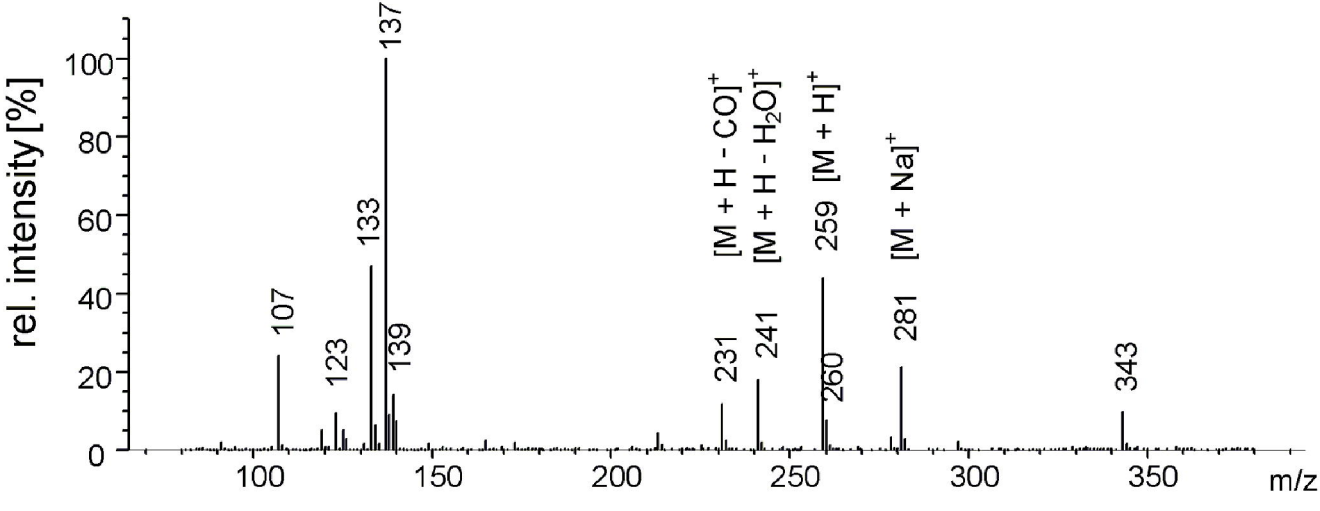
rel. intensity [%]
100
80
60
40
20
0
100
150
200
250
300
350
m/z
107
123
133
137
139
231
[M + H - CO]+
241
[M + H - H2O]+
259
[M + H]+
260
281
[M + Na]+
343

Figure 12

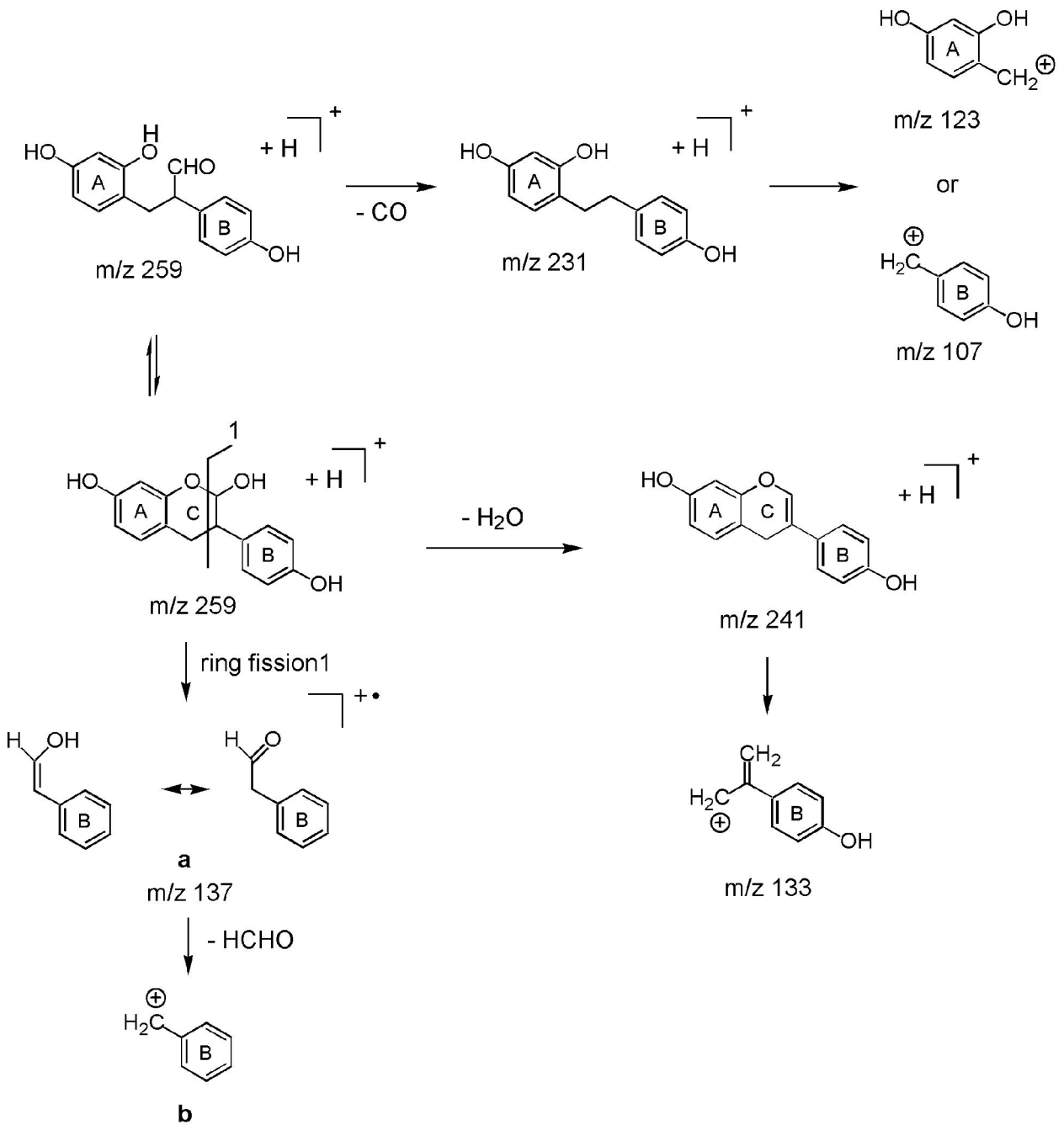
HO
OH
A
CH2
m/z 123
or
H2C
B
OH
m/z 107
m/z 259
- CO
m/z 231
1
C
- H2O
m/z 241
ring fission1
H
O
a
m/z 137
- HCHO
b
m/z 133

Figure 13

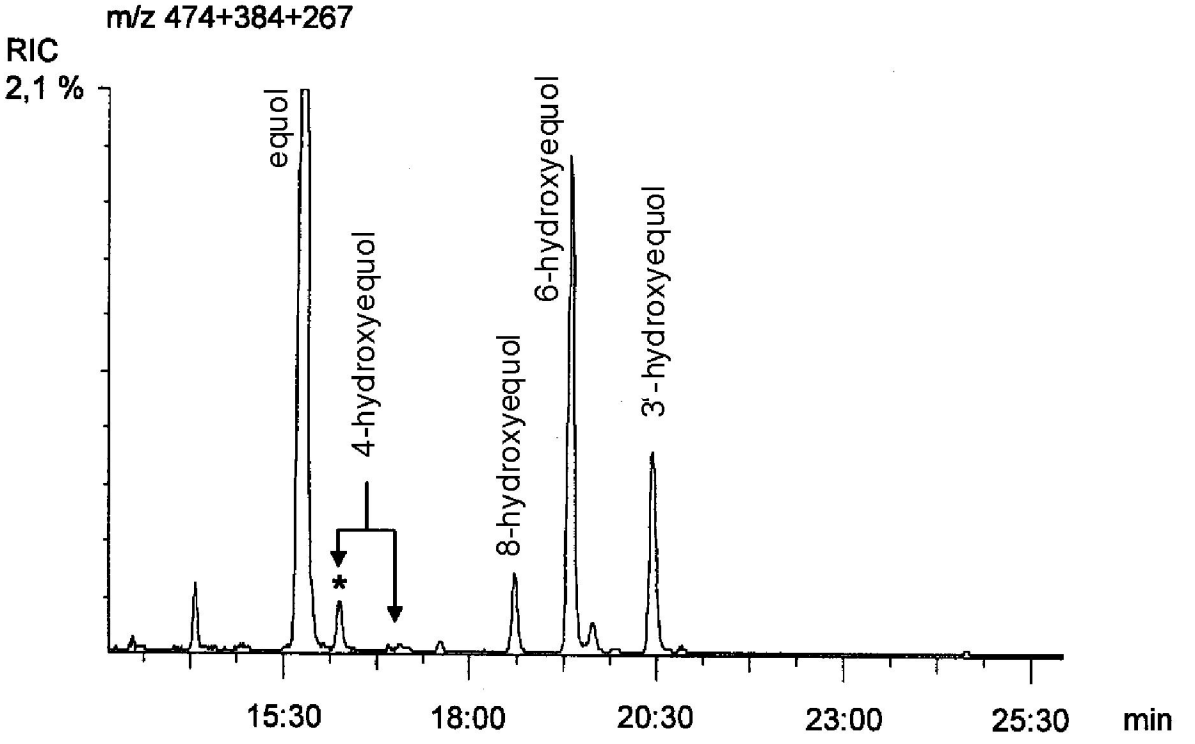
m/z 474+384+267
RIC
2,1 %
equol
4-hydroxyequol
8-hydroxyequol
6-hydroxyequol
3'-hydroxyequol
*
15:30
18:00
20:30
23:00
25:30
min

Figure 14

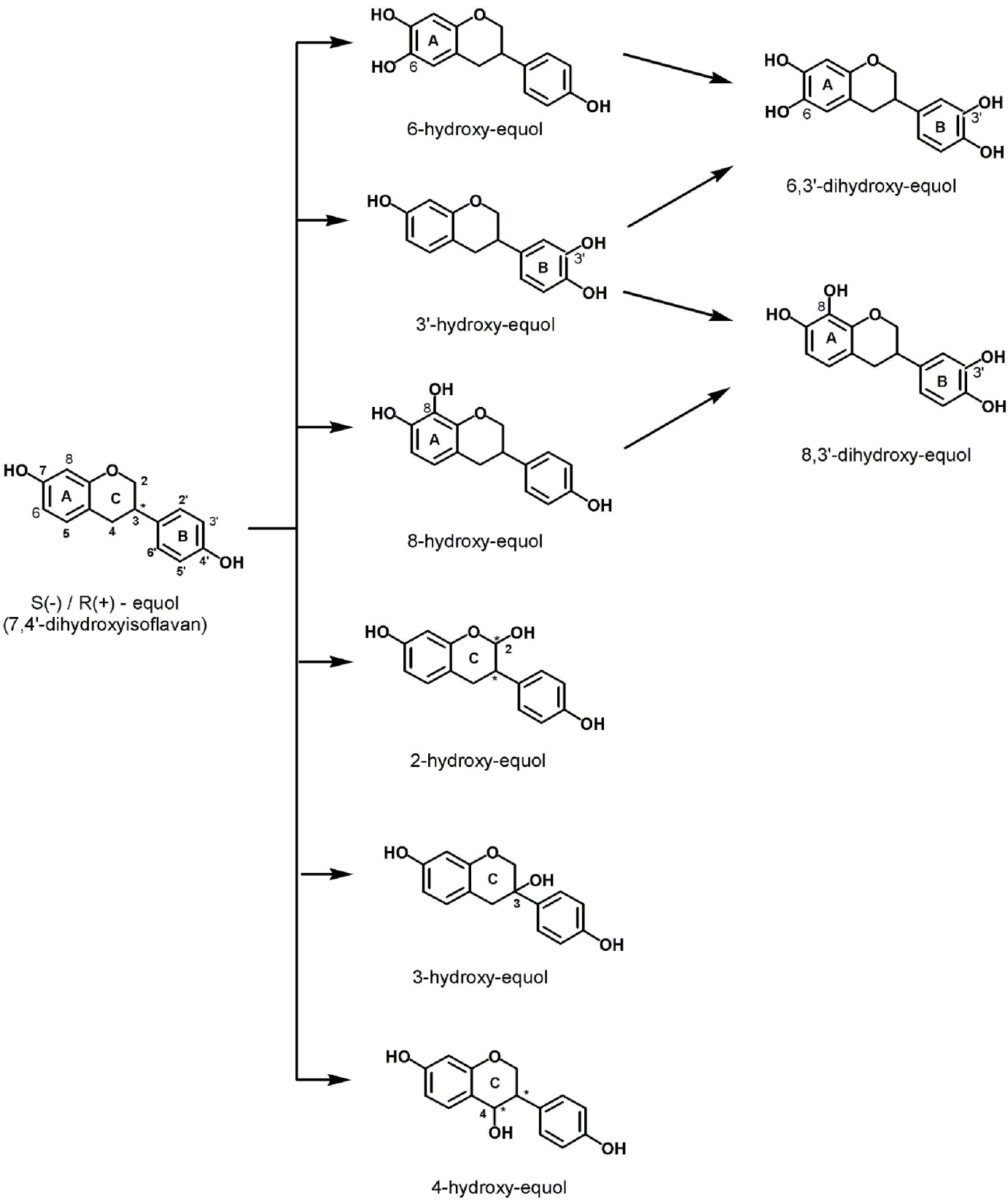
S(-) / R(+) - equol
(7,4'-dihydroxyisoflavan)
6-hydroxy-equol
3'-hydroxy-equol
8-hydroxy-equol
2-hydroxy-equol
3-hydroxy-equol
4-hydroxy-equol
6,3'-dihydroxy-equol
8,3'-dihydroxy-equol

Figure 15

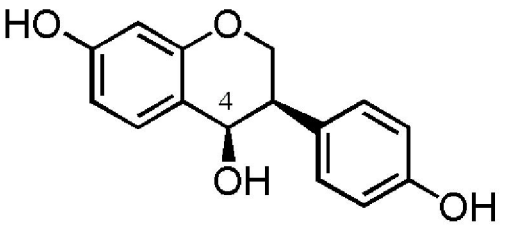

3S,4R-4-hydroxyequol

"cis"

reduction by the gut microflora

stereospecific hydroxylation by cytochrome P450 enzymes

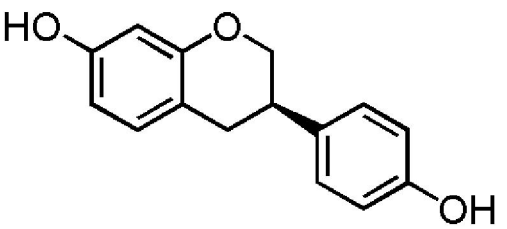

S-(-)-equol